ELSEVIER

Journal of Chromatography A, 914 (2001) 131–145

JOURNAL OF CHROMATOGRAPHY A

www.elsevier.com/locate/chroma

# Separation and quantification of the linear and cyclic structures of polyamide-6 at the critical point of adsorption

Y. Mengerink[a,*], R. Peters[a], C.G. deKoster[a], Sj. van der Wal[a], H.A. Claessens[b], C.A. Cramers[b]

[a]*DSM Research, P.O. Box 18, 6160 MD Geleen, The Netherlands*

[b]*Laboratory of Instrumental Analysis, Eindhoven University of Technology, P.O. Box 513, 5600 MB Eindhoven, The Netherlands*

**Abstract**

The linear and cyclic structures of polyamide-6 were separated by liquid chromatography at critical conditions (LCCC) and identified with different mass spectrometric (MS) techniques and quantitated by LCCC with evaporative light-scattering detection (ELSD). Electrospray ionization MS was not suitable to identify the higher cyclic structures. For this purpose, matrix-assisted laser desorption ionization time-of-flight MS performed better and cyclic and linear structures were oligomerically resolved and separately identified in the mass spectrometer. The highest cyclic structure present and detected was the cyclic pentacontamer. It could be demonstrated that cyclic and linear oligomers follow different ionization and fragmentation routes/patterns. Quantification with ELSD of the components separated by LCCC using a universal calibration curve or an iterative procedure was developed. An area correction to account for different peak widths of coeluting components improves precision and accuracy of the calibration curve and improves quantitation accuracy for the samples analyzed. With these corrected values, no molecular mass dependency was observed for the cyclic and linear structures. Under critical conditions, the linear and cyclic structures of polyamide-6 were separated, identified and quantified. 

*Keywords:* Liquid chromatography at critical conditions; Polyamide

## 1. Introduction

Polyamide-6 is a nylon, based on the monomer caprolactam, which is capable of polymerizing by ring opening at elevated temperatures. Cyclic structures of polyamides can be generated due to intramolecular condensation or to backbiting mechanisms (Fig. 1) [1]. Theoretically, an indication of the amount of cyclic structures in a linear homopolymer can be calculated by comparing the average number molecular mass ($M_n$), obtained e.g. by size-exclusion chromatography [2], by titration for specific endgroup determination [3] or by nuclear magnetic resonance [3,4] for endgroup versus number of backbone units, using Eq. (1):

$$\bar{M}_nE = \frac{\sum_{i=1}^{\infty} n_{iL}M_{iL} + \sum_{i=1}^{\infty} n_{iC}M_{iC}}{\sum_{i=1}^{\infty} n_{iC} + \sum_{i=1}^{\infty} n_{iL}} \cdot \frac{\sum_{i=1}^{\infty} n_{Li}}{\sum_{i=1}^{\infty} n_{Li}M_{Li} + \sum_{i=1}^{\infty} n_{Ci}M_{Ci}} = \frac{\sum_{i=1}^{\infty} n_{Li}}{\sum_{i=1}^{\infty} n_{iC} + \sum_{i=1}^{\infty} n_{iL}} \quad (1)$$

*Corresponding author. Tel.: +31-46-476-1632; fax: +31-46-476-1127.

*E-mail address:* ynze.mengerink@dsm-group.com (Y. Mengerink).

0021-9673/01/$ – see front matter 
PII: S0021-9673(01)00622-7

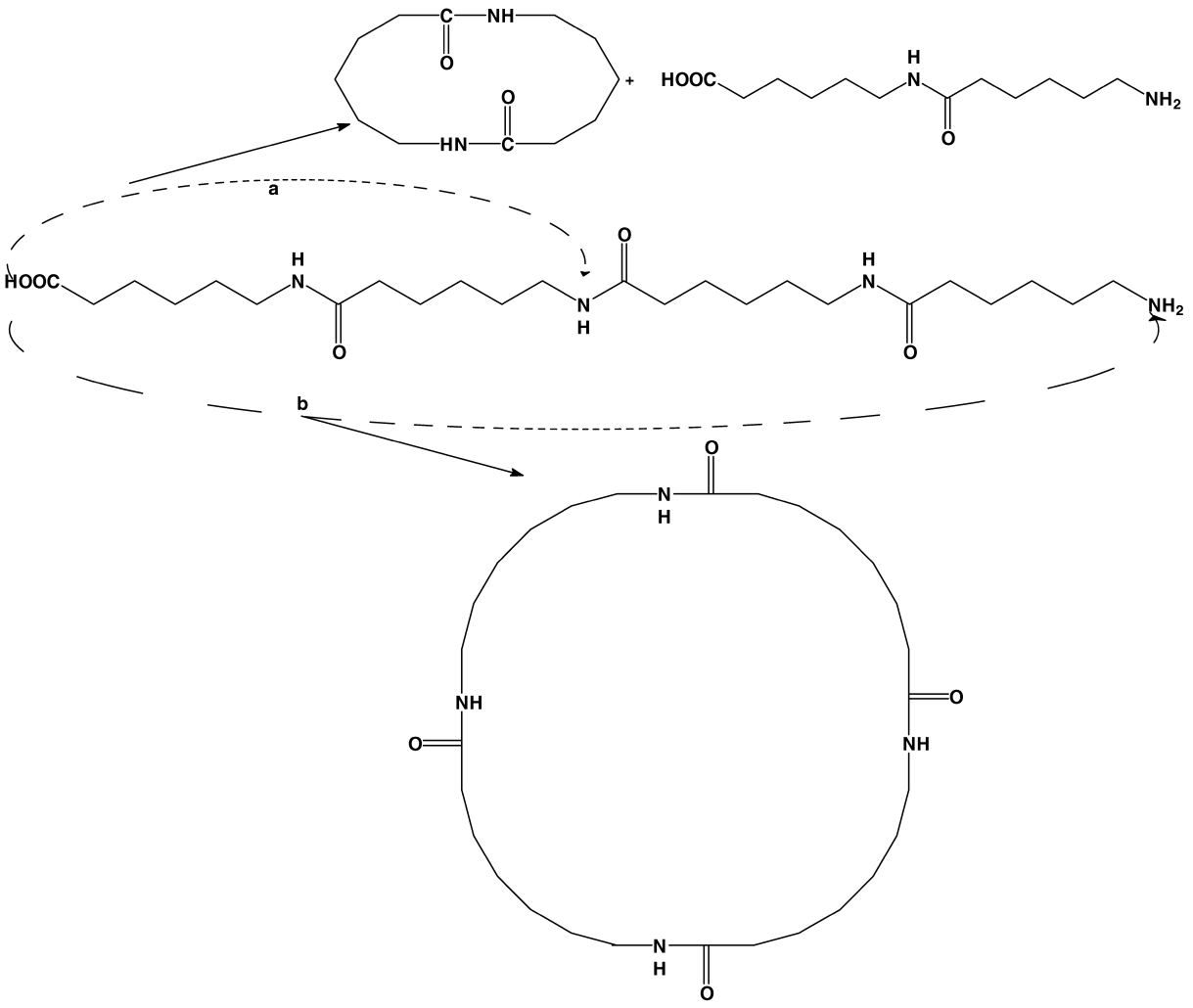


Fig. 1. Creation of cyclic structures from linear tetramer. (a) Formation of cyclic dimer due to backbiting and (b) formation of cyclic tetramer due to intramolecular condensation.

where $M_n$ is the number-average molecular mass in $g\,mol^{-1}$, $E$ is the concentration of a particular endgroup (acid or amine) in equiv. $g^{-1}$, $n$ is the number of linear (L) or cyclic (C) molecules with i backbone units and $M$ is the molar mass of a linear (L) or cyclic (C) molecule with i backbone units. However, in practice this method is not used as it is indirect, only applicable for very well defined homopolymers and only an average number is obtained which does not open the possibility of determining the distributions of the different series. Another technique, with the potential to identify all molecules is matrix-assisted laser desorption ionization time-of-flight mass spectrometry (MALDI-TOF-MS). However, direct quantification of polymer species from MS spectra is questionable [5,6] and the assessment, whether cyclic structures are present or not, could be complicated by the formation of [linear $-H_2O$] ions by postionization decay of the linear oligomers in the ion source of the mass spectrometer. It has been shown that upon MALDI of hyperbranched polyesteramides, a substantial in-source metastable decay of the protonated molecules occurs. This in-source decay led initially to the conclusion that a substantial

part of the polymers studied consisted of cyclic oligomers [7].

In 1986 Entelis et al. demonstrated liquid chromatography at critical conditions (LCCC) [8]. In the size-exclusion mode the higher-molecular-mass polymer is excluded from the pores and will therefore elute before the lower-molecular-mass polymer (see Fig. 2, left curve). However, when the separation conditions favor adsorption, the higher-molecular-mass polymer will elute after the low-molecular-mass polymer, because the high-molecular-mass polymer contains more backbone units, which interact with the stationary phase (Fig. 2, right curve). Under certain conditions, which are critical with respect to temperature and mobile phase composition, both effects compensate each other and retention becomes independent of the molecular mass and is solely governed by endgroup functionality (Fig. 2, middle curve). A number of papers have been published to demonstrate the use [9–17] and problems [18,19] of this technique. Although the critical conditions of linear structures are not exactly the same as for cyclic structures [8], the feasibility of separating these kinds of macromolecules independently of their molecular mass has been demonstrated for polyethers [8,20–22] and polyesters [23,24].

Since standards of higher cyclic oligomers of polyamide-6 are not available to characterize the peak, identification of this group of components is necessary. Due to its simplicity, on-line LC-electrospray ionization (ESI) MS is the first choice to verify whether a particular group of components is cyclic. However, due to its inherent higher mass range and ability to generate singly charged ions, MALDI-TOF-MS could be used to characterize higher oligomeric and polymeric structures [25,26]. Some experimental set-ups demonstrated the possibility of on-line coupling of MALDI-TOF-MS with an LC system [27–29]. However, in practice MALDI-TOF-MS is usually coupled off-line to critical LC systems [21].

Although ESI-MS and MALDI-TOF-MS are very suitable for identification purposes, they are unsuitable for quantitative analyses in critical chromatography. If UV detection can be used, this is of course the method of choice, as often the contribution of a monomeric unit can be used to calculate the mass percentages of the different functional polymers [30]. However, if no chromophores are available or if background absorption is too high, evaporative light scattering detection (ELSD) can be used instead, although its non-linear behavior gives some bias.

Quantification after a critical separation is not straightforward. Within a particular series, but also for different separated series, low-molecular-mass molecules with other molecules could give different response factors. Quantification methods are often not given in the literature and the problem described above is usually ignored [20,23,31,32]. Pasch et al. compared refractive index detection after a critical separation with the summed amounts measured with

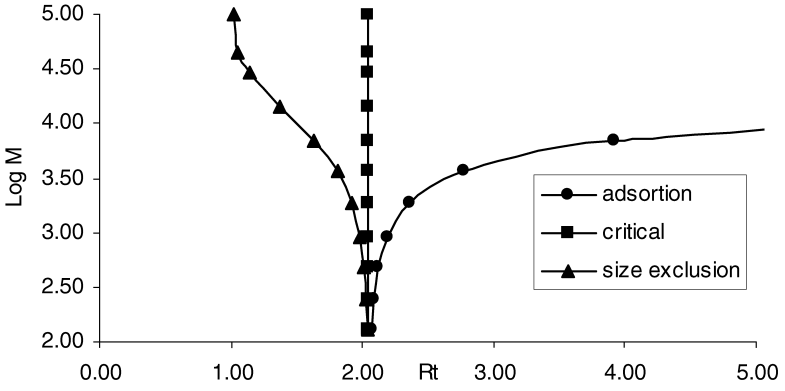


Fig. 2. Three modes of chromatography. (a) Size-exclusion (triangles), where higher-molecular-mass polymers have decreased elution times; (b) adsorption (circles), where the higher-molecular-mass polymers have increased elution times and (c) critical conditions (squares), where retention is independent of the molar mass. $t_R$, Retention time in min.

supercritical fluid chromatography and found good quantitative correlations between the different techniques [21]. However, this is not in agreement with the molecular mass dependence of response, as given by the same author [21]. Beside this, the refractive index detector is not very sensitive and suffers from baseline disturbances in the elution window of the critical separation [21]. For some examples, Pasch et al. also mentioned the best, but most tedious way to calibrate: preparative isolation of the separated peaks to use them as standards [21]. This time consuming procedure can only be used when the recovery of the work-up procedure is investigated. For another sample, the distribution of the particular series should be investigated or another preparative isolation should be performed.

Here we demonstrate the potential power of LCCC for the separation of linear and cyclic structures of polyamide-6 (Fig. 1). Furthermore, we discuss the use of different MS techniques for identification purposes and develop a method to use ELSD for quantification.

## 2. Theory

One of the major drawbacks of the ELSD is its non-linear behavior. An exponential calibration curve, such as given in Eq. (2), is often used:

$$\text{Area} = A_0' m_{\text{inj}}^{A_1} \tag{2}$$

where the area is correlated to the injected mass with the constants $A_0'$ and $A_1$.

If the response of different compounds (e.g. the linear versus cyclic structures) is similar and the peak widths are uniform, Eq. (2) can be used for a universal calibration. However, due to differences in molecular mass (cyclic predominantly low molecular mass versus linear predominantly high molecular mass), peak widths are often not the same and a correction should be made to increase accuracy.

Fundamentally, the response equation should be written as:

$$\text{response}(t) = A_0 c(t)^{A_1} \tag{3}$$

where response($t$) and $c(t)$ are the detector response and the concentration of the solute at time $t$.

For a Gaussian peak, the concentration at time $t$ is given as [33]:

$$c(t) = \frac{m_{\text{inj}}}{F\sqrt{2\pi\sigma}} \cdot \mathrm{e}^{-\frac{(t-t_r)^2}{2\sigma^2}} \tag{4}$$

where $c(t)$ is the concentration at time $t$, $m_{\text{inj}}$ is the injected mass, $F$ is the flow-rate, $t_{\text{R}}$ and $\sigma$ the retention time and standard deviation of the peak. To obtain the area of a peak, the response $c(t)$ must be integrated over the time (zero to infinity) and in combining with Eqs. (3) and (4) this yields [34]:

$$\begin{aligned}\text{Area} = A_{\text{o}} \cdot \left(\frac{m_{\text{inj}}}{F\sqrt{2\pi\sigma}}\right)^{A_1} \\ \cdot \left[\sqrt{\frac{\sigma^2\pi}{2A_1}} \cdot \text{erf}\left(\sqrt{\frac{A_1}{2\sigma^2}} \cdot (\infty - t_{\text{R}})\right)\right. \\ \left. -\sqrt{\frac{\sigma\pi}{2A_1}}\,\text{erf}\left(\sqrt{\frac{A_1}{2\sigma^2}}(0 - t_{\text{R}})\right)\right]\end{aligned} \tag{5}$$

This equation can be simplified dramatically and it can be easily deducted that:

$$\text{Area} = A_{\text{o}}\sqrt{\frac{2\pi}{A_1}} \cdot \frac{\sigma^{(1-A_1)}}{(F\sqrt{2\pi})^{A_1}} \cdot m_{\text{inj}}^{A_1} \tag{6}$$

Eq. (6) gives the peak width (and flow) dependence of the area-injected mass correlation. It can also be seen that the power-constant $A_1$ used in Eqs. (2) and (3) is the same. However, $A_0'$ of Eq. (2) is not equal to $A_0$ in Eq. (3). Their correlation is given by [35]:

$$A_0^1 = A_{\text{o}}\sqrt{\frac{2\pi}{A_1}} \cdot \frac{\sigma^{(1-A_1)}}{(F\sqrt{2\pi})^{A_1}} \tag{7}$$

In practice two peaks can be compared, or the area of multiple peaks can be converted to normalized peak areas with a standard deviation of e.g. unity.

To correct for peakwidth dissimilarities, the area of a peak should be corrected to a normalized area with a standard peakwidth. Combining Eqs. (2) and (6) can perform this correction:

$$\text{Area}\,(a) = \text{area}\,(b) \cdot \left(\frac{\sigma_a}{\sigma_{\text{b}}}\right)^{(1-A_1)} \tag{8}$$

where area ($a$) is the normalized area ($b$), $\sigma_{\text{a}}$ is the standard deviation of the normalized peak, which can be set arbitrarily, $\sigma_{\text{b}}$ is the standard deviation of the peak which has to be normalized and $A_1$ is the

constant of the calibration curve (see Eqs. (2) and (3)).

## 3. Experimental

All experiments were performed on a HP1100 quartenary pump, including a degasser and a control module (Hewlett-Packard, Waldbronn, Germany,) The mobile phase, formic acid–1-propanol (81.6:18.4, w/w), was premixed and pumped with a flow-rate of 0.65 ml/min. Two 200×4 mm Nucleosil 50-5 (Macherey-Nagel) columns were used to perform the critical separation.

The injector (Rheodyne, Cotati, CA, USA), equipped with a 55-μl loop, was mounted inside the column oven at 38°C (Mistral, Spark, The Netherlands). Approximately 6 m of 0.25 mm I.D. capillary was used in this oven to thermostate the mobile phase before it reached the injector. Detection with the Sedex 55 ELSD system (Sedere, Vitry/Seine, France) was performed with an optimized drift tube temperature of 55°C and 1.9 bar air pressure. The detector signal, areas and peak width were all collected with an X-CHROM/WINDOWS NT 3.51 version 2.11b data management system (Lab-systems, Manchester, UK).

Data calculations were performed using a spreadsheet program (EXCEL 97, Microsoft). Default values of the SOLVER (EXCEL97 subroutine), to solve problems iteratively, are Max time:100 s; iterations 100; precision 0.000001; tolerance 5%; convergence 0.001%; estimates: tangent; derivatives: forward; search: Newton.

LC–ESI(+)MS was performed on a HP1100 quaternary pump, including a degasser and a Chemstation (A.06.03) (Hewlett-Packard); $m/z$ range 100–1500 (step 0.1, data storage: full), fragmentor = 100 V, $V_{cap}$ = 3 kV, drying gas 10.0 l $min^{-1}$ $N_2$, nebulisation pressure 50 p.s.i.g. (1 p.s.i. = 6894.76 Pa).

MALDI-TOF-MS was carried out using a Perkin-Elmer/PerSeptive Biosystems Voyager-DE-RP MALDI-TOF mass spectrometer (PerSeptive Biosysytems, Framingham, MA, USA) equipped with delayed extraction [36]. A 337-nm UV nitrogen laser producing 3 ns pulses was used and the mass spectra were obtained in the linear and reflectron mode. Samples were prepared by mixing 10 μl of hexafluoroisopropanol (HFIP) solution of the polyamide fractions with 30 μl of a solution of 3 mg $l^{-1}$ 2,5-dithranol in HFIP. A 1-μl volume of that solution was loaded on the gold-sample plate. The solvent was removed in warm air.

All oligomers and polyamides used were synthesized at DSM, except polyamide-6 (PA-6) 16 kD, PA-6 24 kD and PA-6 35 kD, which where purchased from Polysciences (Warrington, PA, USA). The linear oligomers are abbreviated by L*n*, the cyclic oligomers by C*n*, where *n* is the number of ($COC_5H_{10}NH$) units (Fig. 1). All samples were dissolved in the mobile phase. The dissolution of the polyamides in formic acid was performed in a Bransonic Ultrasonic cleaner Model 5210 (Danbury, CT, USA).

## 4. Results

### 4.1. Separations under critical conditions

Critical conditions are often not easy to find. The availability of well-defined polymers at different molecular masses will simplify this task. Although laboratory-made linear oligomers and polymers of 6-aminocaproic acid are available at all kinds of different molecular masses, their cyclic forms are only available at low molecular masses ($n$ = 1–10). With the use of a low- and a high-molecular-mass linear polymer, conditions have to be found where both samples coelute. If the higher-molecular-mass sample elutes before the lower-molecular-mass sample (i.e. the SEC mode) the strong solvent concentration should be decreased. If the retention times match each other closely, temperature can be used for fine-tuning. Again, in the SEC mode, temperature should be decreased to approach the critical conditions. As true critical conditions are hard to obtain, it is advisable to work at very slight exclusion conditions, as this will enhance recovery. A representative chromatogram is given in Fig. 3. The chosen conditions were based on a normal-phase system, with formic acid as a good solvent for polyamide-6. 1-Propanol was used as a relatively non-polar non-solvent. With the available lower cyclic components, the second peak was identified as cyclic polyamide-6 components. However, higher

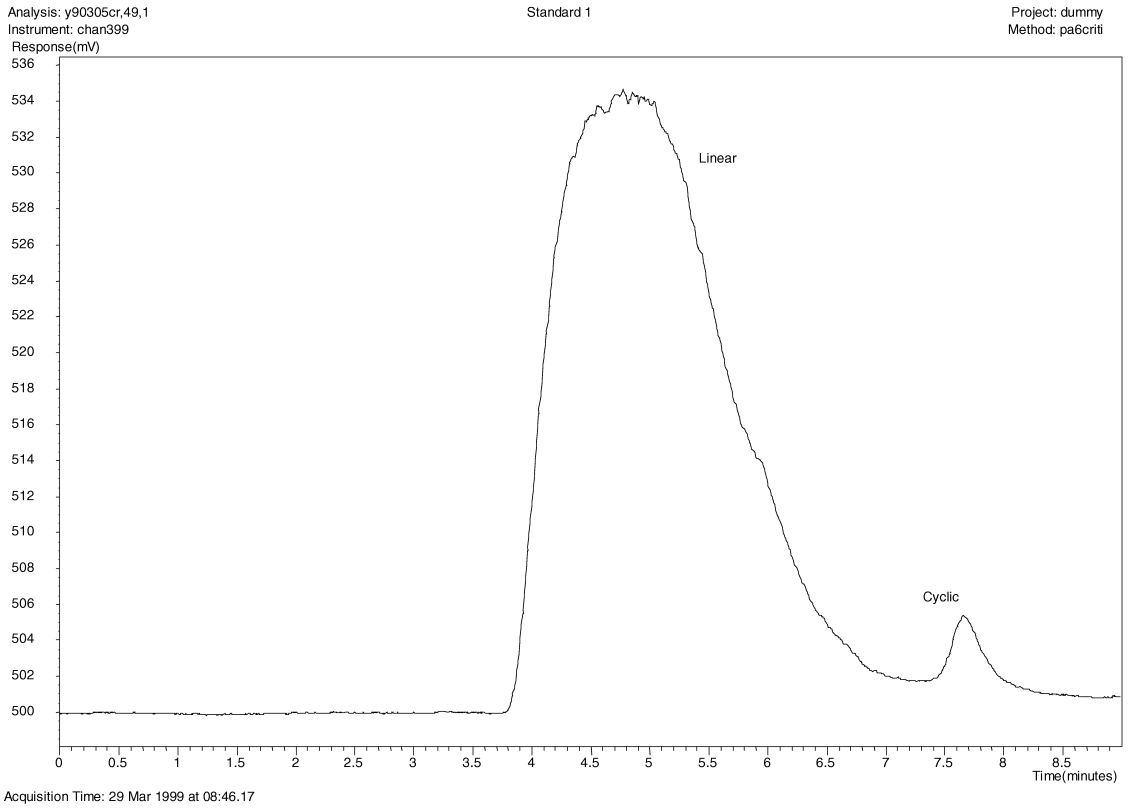


Fig. 3. Chromatography of a typical polyamide-6 sample under near critical conditions: Mobile phase: 0.65 ml $min^{-1}$ of 81.6% (w/w) formic acid in 1-propanol. Endgroup functional separation on 2×(200×4 mm) Nucleosil 50-5 at 38°C, 55 μl injected of a PA-6 sample dissolved in mobile phase. Detection: ELSD, 55°C 1.9 bar nebulisation air pressure. [Total permeation volume was 3.9 ml (linear monomer), and the elution volume for PA-6 36=3.1 ml].

cyclic structures were not available, making selective MS identification of the second peak necessary to demonstrate true critical conditions for all cyclic structures.

### *4.2. Identification by ESI-MS*

With on-line coupled LC–ESI-MS, the low-molecular-mass cyclic structures ($n < 11$) could easily be identified. Fig. 4 depicts the different elution behavior of the cyclic monomer compared to the cyclic oligomers, which can be explained by its high dipole moment [37,38]. In Fig. 5a the ESI-MS spectrum of the second (cyclic) peak is given. However, mass resolving power problems arise for higher-molecular-mass structures, as can be seen in the MS spectrum of the first (linear) peak (Fig. 5b). ESI of polyamides generates multiply charged molecules with a broad charge distribution. The maximum of the charge distribution of such a molecule depends on the number of basic sites for protonation, e.g. a 500-mer may have a distribution with a range from one up to five-hundred positive charges. A 500-mer with five-hundred charges will yield a nominal mass peak at $m/z$ 114 in the mass spectrum. This nominal peak has to be convoluted with the natural isotope distribution of a 500-fold protonated 500-mer [39–41]. As high-molecular-mass components can only be characterized by multiply charged ions, it can be anticipated that deconvolution is almost impossible for broadly distributed polymers in the same mass range. At the higher range of the molecular mass distribution of a representative polyamide, the molar mass distribution of a single linear

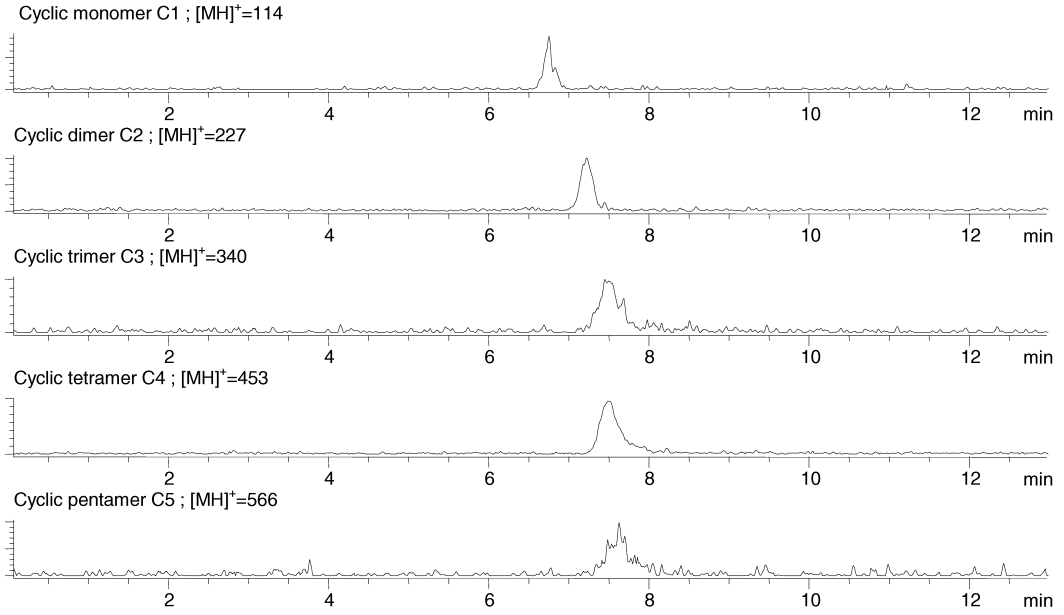


Fig. 4. Chromatography of cyclic oligomers of PA-6 under critical conditions: Mobile phase: 0.65 ml $min^{-1}$ of 81.6% (w/w) formic acid in 1-propanol. Endgroup functional separation on 2×(200×4 mm) Nucleosil 50-5 at 38°C, 1 μl injected of different cyclic PA-6 oligomers (approx. 0.1 mg/ml), dissolved in mobile phase. Detection: ESI(+)-MS.

500-mer molecule (containing 3000 carbon atoms) is, due to the C13-contribution, already very broad (Fig. 6). If this molecule contains 500 protons $[MH_{500}]^{500+}$ it will give a signal not only at [M/500+1] and its corresponding $C_{13}$ isotope, but also at all decimal masses in between. In the $m/z$ range of 500–1000 and $z = 56–113$ this molecule with the mean mass of 56 580 g $mol^{-1}$ will already give approximately 1500 different abundances in the mass spectrum. In conclusion, multiple charging leads to a molecular mass distribution which is convoluted by numerous charge distributions and isotope distribution. Thus, peaks at almost every $m/z$ value of the mass spectrum are obtained. As can be seen in Fig. 5b an understandable but unreadable spectrum appears.

### *4.3. Identification by MALDI-TOF-MS*

For the identification of higher-molecular-mass polyamides MALDI-TOF-MS is more suitable than ESI-MS. Generally MALDI produces singly charged oligomers/polymer and as a result the molecular mass distribution is not convoluted by a charge distribution leading to mass resolving resolution problems as observed in the ESI spectra (see above). Moreover, the TOF mass analyzer allows detection of high-molecular-mass singly charged oligomer species. Improvements in matrix and sample preparation strategies have extended the molecular mass range for analysis of synthetic polymers by MALDI up to $1.5 \cdot 10^6$ [42].

With preparative LCCC the two peaks were fractionated. The purity of the collected fractions was determined by liquid chromatography [43,44]. No cross-contamination of the linear and cyclic components was observed. The collected fractions were analyzed with MALDI-TOF-MS. In Fig. 7 the MALDI-MS spectrum (linear mode) of the second cyclic peak is given. The corresponding spectra of fractions of the first peak showed a small mass dependence, indicating near-critical conditions. It can also be concluded that the MALDI efficiency for a single protonated cyclic molecule is much higher as compared to the ESI.

A series of structurally related homologous oligomers could be discerned on the basis of the MALDI-TOF-MS spectrum. The strategy used for the identi-

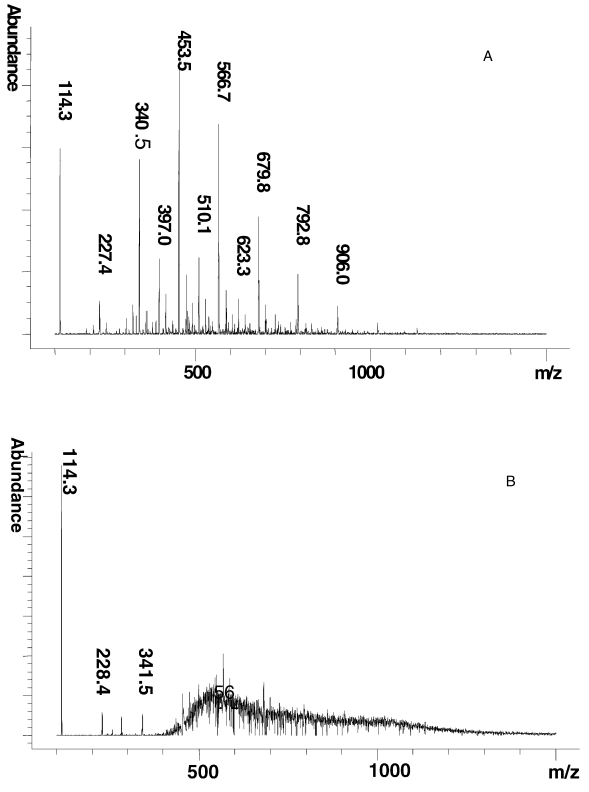


Fig. 5. LC–ESI-MS spectra of linear and cyclic structures. (a) Cyclic structures; (B) linear structures.

fication of the protonated/cationized oligomers and for determination of the chemical composition of the individual oligomers by extrapolation to zero oligomers has been discussed elsewhere [45,46]. This strategy has been applied in this study without any modification. One series of pseudomolecular ions in the spectrum of the first peak in the chromatogram with a mass increment of 113 confirms the caprolactam repeating unit. Extrapolation to zero monomers gives a residual mass of 19. This residual mass is the summation of the end-group mass and the mass of the ionizing species. The end-group and ionizing species for this series of homologous oligomers are a water molecule (molecular mass 18) and a proton, respectively. The spectrum is characteristic for PA-6 linear oligomers. Analogous results are obtained for the oligomer distribution of the second peak (depicted in Fig. 7). In this case, extrapolation to zero oligomers leads to the identification of protonated oligomers with a zero end-group mass, i.e. protonated cyclic oligomers.

To investigate the spectra of the two series of oligomeric peaks in more detail, MALDI in the reflectron mode was used to study the linear (Fig. 8a) and cyclic nonamer (Fig. 8b). Mass analysis in reflectron mode was carried out to obtain spectra with sufficient resolution to resolve the individual

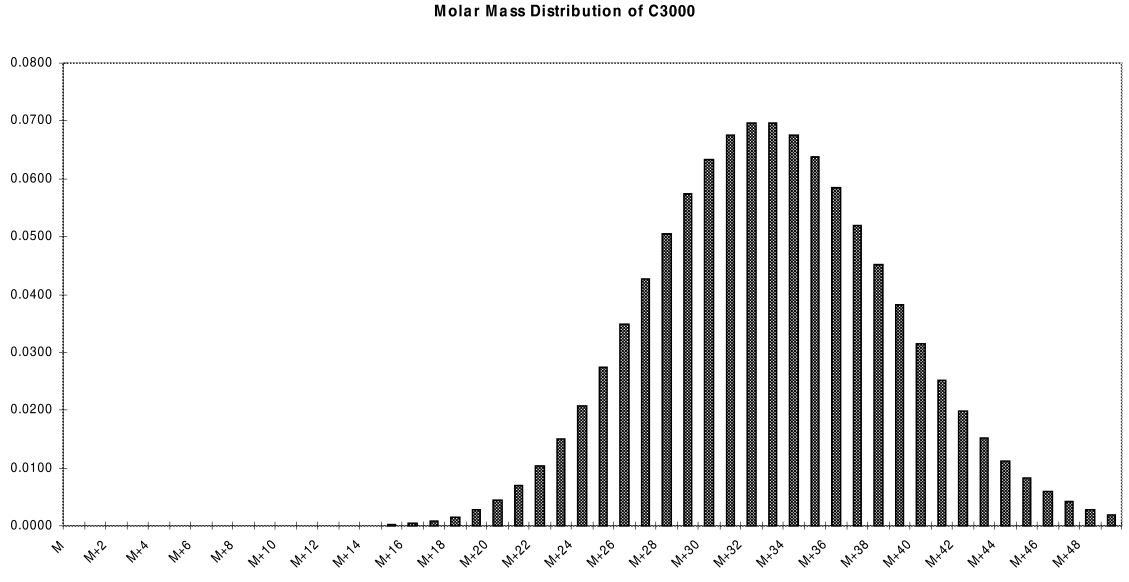


Fig. 6. Distribution of molar mass of a molecule containing 3000 $^{12}C$ atoms.

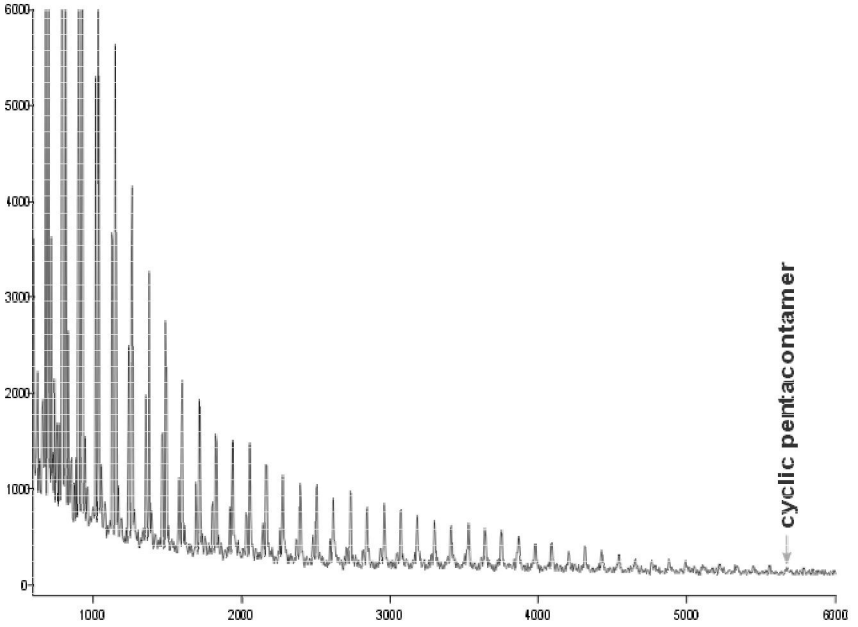


Fig. 7. MALDI-MS spectrum (linear mode) of the second peak (cyclic structures).

$^{13}C$ isotopes. The dominant mode of ionization of the polyamide oligomers under the experimental conditions applied is metal ion attachment. Sodium cationization of the linear nonamer leads to the formation of $m/z$ 1058 $[M+Na]^+$ pseudomolecular ions. Potassium cationized species are observed at $m/z$ 1074 $[M+K]^+$. Protonation yields cations at $m/z$ 1036 $[M+H]^+$. The pseudomolecular ions of the polyamide oligomers are readily recognized by this characteristic $m/z$ $[M+H]^+$, $m/z$ $[M+Na]^+$ and $m/z$ $[M+K]^+$ peak pattern. The $m/z$ 1040 is formed by metastable fragmentation of the cationized linear nonamer in the mass spectrometer [7]. The peaks in the MALDI spectrum of the cyclic nonamer are assigned as $m/z$ 1018 $[M+H]^+$, $m/z$ 1040 $[M+Na]^+$ and $m/z$ 1056 $[M+K]^+$.

### *4.4. Quantification with ELSD*

ELSD could be sensitive to molecular mass and chemical composition as both may influence the time to complete evaporation, as indicated by Charlesworth [47]. However, in practice it is almost impossible to use a calibration standard with the same molecular mass distribution as the investigated polymer. To investigate the validity of Eq. (8) and the possibility of molecular mass dependence, a universal calibration curve was constructed by injecting ten different kinds of polyamides on the critical system. Five samples of cyclic oligomers and five samples of linear oligomers/polymers with different molecular masses were investigated. Only samples with no significant contamination of the opposite structure were used (Table 1). Due to its relatively low melting and boiling points (Table 2), the cyclic monomer caprolactam did not yield any response. On the other hand, the linear monomer was more sensitive than the other components and therefore both monomers were excluded from the calculation of the universal calibration curve.

In practice, this is a minor problem, as the linear monomer is only present in the low ppm range (often $<5$ mg/kg polyamide-6 [30]. The amount of cyclic monomer is relatively high in unwashed polyamide and should be determined separately [30,37,43]. In Fig. 9, the natural logarithm of the injected mass is plotted against the natural logarithm of the area and the corrected area. The subsequent statistical data are given in Table 3. From Fig. 9 together with the correlation coefficients (Table 3) and the standard

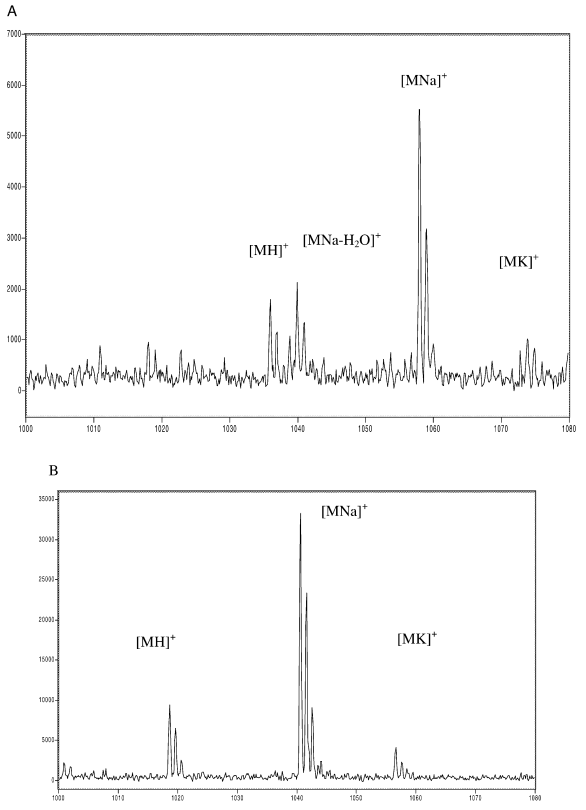


Fig. 8. MALDI-MS spectra (reflection mode) of (A) the first peak (focused on the linear nonamer) and (B) the second peak (focussed on the cyclic nonamer).

deviation of the $\Delta m_{inj}$ values (Table 1), it can be concluded that peak width–area correction improves precision of the universal calibration curve. The different distributions of these samples do not influence this curve. From Fig. 10 it can also be concluded that the accuracy improves, as due to the area–peak width correction the deviation in weighted amount versus calculated amount decreases. It can be anticipated that a peak width–area correction of a real sample will improve accuracy. Four different polyamides were analyzed under critical conditions with ELSD as an universal detection method. To determine the percentage cyclic (%C), different procedures can be followed. First, the universal calibration curve as discussed above, can be used to determine the absolute amount of linear polymer and cyclics. The amount of cyclics can now be calculated compared to the original mass of the sample or compared to the sum of the percentages linear polymer and cyclics calculated.

In Table 4 the concentration of cyclic components is given by using the universal calibration curve. Recoveries of 94% or more are obtained with all samples, except for the PA-6 24, where recovery is only 84%. A high content of a volatile component or the presence of non-eluting contaminations may cause this. From the results of Table 1 and the recoveries of Table 4 no significant molecular mass dependence was observed. If calibrants are not available to construct such a universal calibration curve the total normalized area sum can be considered as the total amount of polymer. With different concentrations injected, an iterative process can be used to determine the different unknowns ($A_0'$; $A_1$ and %C). With an iterative procedure, one should be aware of the strategy used. The starting values are important. An easy way to obtain these initial values is to construct curves of the natural logarithm of the injected polymer mass $m_{inj}$ versus the natural logarithm of the non-corrected areas of the linear and cyclic peaks. The slope of these two curves ($=A_1$) will be approximately the same. The average value can be used as the initial $A_1$ value to start the iteration process. The intercept of the linear regression curve of the linear oligomers/polymer ($=\ln A_0'$) can be used to calculate the initial value of $A_0'$. Predictions about the percentage cyclic (%C) can be made, by comparing the areas of the chromatogram. In our iterative optimization procedures, different initial %C values were used. A good optimization value is the summated $\chi^2$ value [48]. We defined $\chi^2$ as:

$$\chi^2 = \sum_{\text{all-peaks}} \frac{(m_{\text{inj-predicted}} - m_{\text{inj-calculated}})^2}{\text{average}\,(m_{\text{inj-predicted}}; m_{\text{inj-calculated}})} \quad (9)$$

$m_{inj-predicted}$ is the predicted value, which can be obtained by multiplication of the $m_{inj}$ with the predicted percentage of the linear (100−%C) or cyclic (%C). $m_{inj-calculated}$ is the calculated amount of the linear or cyclics components, using the normalized areas (Eq. (8)) and the predicted $A_0'$ and $A_1$ values. Thus, if the %C, $A_0'$ and $A_1$ are predicted, the $\chi^2$ value of all peaks can be calculated. The iterative optimization procedure works best, if all

Table 1
Overview of the calculated and peak width corrected injected masses of ten different species[a]

| | $m_{inj}$ (μg) | Area counts (mV s) | $\sigma$ (s) [$\Delta s$ in %] | $m_{inj}$ calc. with universal calibration (μg) | $\Delta(m_{inj})$ (%, w/w) | Area corrected to $\sigma=1$ | $m_{inj}$ calc. with corrected area | $\Delta(m_{inj})$ corrected (%, w/w) |
|---|---|---|---|---|---|---|---|---|
| C ($n=2$) | 3.42 | 1050 | 6 [−4] | 3.99 | 17 | 1450 | 3.54 | 3 |
| C ($n=2$) | 7.02 | 2700 | 5 [0] | 8.76 | 25 | 3600 | 7.61 | 8 |
| C ($n=2$) | 38.0 | 19 000 | 6 [9] | 47.0 | 24 | 26 500 | 40.5 | 6 |
| C ($n=3$) | 5.34 | 1500 | 7 [−3] | 5.30 | −1 | 2050 | 4.79 | −10 |
| C ($n=3$) | 2.08 | 470 | 7 [−5] | 1.98 | −5 | 655 | 1.84 | −12 |
| C ($n=4$) | 3.51 | 895 | 8 [−7] | 3.43 | −2 | 1300 | 3.24 | −8 |
| C ($n=4$) | 11.7 | 4350 | 8 [−2] | 13.0 | 13 | 6200 | 12.0 | 2 |
| C ($n=4$) | 31.0 | 14 500 | 7 [−2] | 37.2 | 20 | 20 500 | 32.6 | 5 |
| C ($n=2$–10) | 1.79 | 345 | 14 [11] | 1.52 | −15 | 540 | 1.57 | −13 |
| C ($n=2$–10) | 11.1 | 4400 | 12 [6] | 13.3 | 20 | 6700 | 12.8 | 16 |
| C ($n=2$–10) | 25.2 | 12 500 | 11 [5] | 32.3 | 29 | 18 500 | 30.2 | 20 |
| C ($n=2$–10) | 67.0 | 34 000 | 11 [23] | 77.3 | 15 | 52 000 | 71.5 | 7 |
| L 1 | 2.86 | 1500 | 5 [0] | 5.31 | 86 | 1950 | 4.61 | 61 |
| L 1 | 11.0 | 7700 | 5 [−4] | 21.5 | 95 | 10 000 | 18.2 | 65 |
| L ($M_w$ 2000) | 2.34 | 625 | 10 [−1] | 2.51 | 7 | 925 | 2.45 | 5 |
| L ($M_w$ 2000) | 25.8 | 11 000 | 12 [−4] | 28.6 | 11 | 16 500 | 27.2 | 5 |
| L ($M_w$ 2000) | 46.1 | 21 500 | 12 [−2] | 51.5 | 12 | 32 500 | 48.3 | 5 |
| L ($M_w$ 5000) | 1.64 | 415 | 30 [30] | 1.78 | 9 | 745 | 2.04 | 25 |
| L ($M_w$ 5000) | 14.0 | 3800 | 25 [5] | 11.7 | −16 | 6550 | 12.6 | −10 |
| L ($M_w$ 5000) | 75.2 | 32 000 | 28 [1] | 72.2 | −4 | 56 500 | 76.3 | 1 |
| L ($M_w$ 8000) | 6.41 | 1600 | 39 [4] | 5.60 | −13 | 2950 | 6.51 | 2 |
| L ($M_w$ 8000) | 27.2 | 8850 | 33 [−3] | 24.2 | −11 | 16 000 | 26.7 | −2 |
| L ($M_w$ 8000) | 63.6 | 22 800 | 38 [3] | 54.5 | −14 | 42 500 | 60.5 | −5 |
| L ($M_w$ 15 000) | 2.48 | 535 | 33 [−54] | 2.20 | −11 | 970 | 2.55 | 3 |
| L ($M_w$ 15 000) | 12.0 | 2750 | 37 [−16] | 8.97 | −25 | 5100 | 10.3 | −14 |
| L ($M_w$ 15 000) | 23.0 | 5950 | 39 [−7] | 17.3 | −24 | 11 000 | 19.7 | −14 |
| L ($M_w$ 15 000) | 85.0 | 27 900 | 48 [−3] | 64.6 | −24 | 54 100 | 73.8 | −13 |
| | | | | $s(\Delta(m_{inj}))$ | 17 | | $s(\Delta(m_{inj,corr})$ | 10 |

[a] $\Delta s$ in %, difference in percentage of $\sigma$, which is the mean value of the converted values of peak width at half height and at $4\sigma$; $M_w$, weight-average molecular mass.

Table 2
Compounds, molecular masses and melting temperatures

| Compound | Molecular mass | Melting temperature (°C) | Boiling temperature (°C) |
|---|---|---|---|
| C1: cyclic monomer | 113 | 69.5 | 139 |
| C2: cyclic dimer | 226 | 348 | |
| C3: cyclic trimer | 339 | 247 | |
| C4: cyclic tetramer | 452 | 261 | |
| C5: cyclic pentamer | 565 | 253 | |
| L1: linear monomer | 131 | 202 | |
| PA-6: polyamide-6 | $10^4$–$4\cdot10^4$ | 220 | |

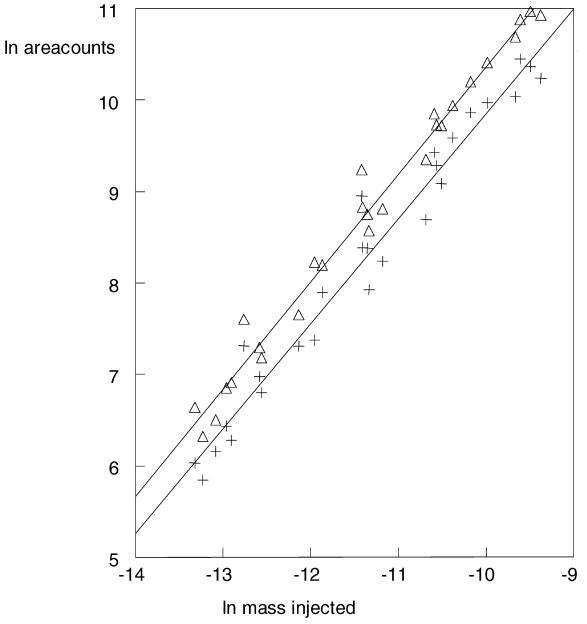


Fig. 9. Influence of peak width correction on the precision of the universal calibration curve. Uncorrected data (crosses) and corrected data (triangles).

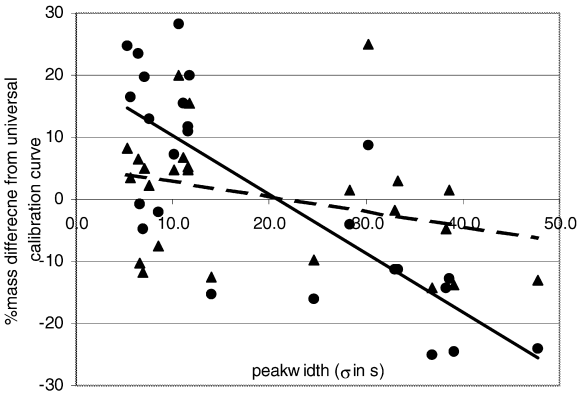


Fig. 10. Influence of peak width correction on accuracy of the calibration curve. Uncorrected data (circles) versus corrected data (triangles).

optimization values ($A_0'$, $A_1$ and %C see Section 4.4) are of the same order of magnitude. This is not the case, and for this reason, the $A_0'$ value is divided by $10^{10}$ and the $\chi^2$ value is multiplied by $10^{10}$. Calculations have to be corrected for $A_0'$, which is not necessary for the $\chi^2$ value. First $A_0'$ and $A_1$ were optimized by minimizing the $\chi^2$. Thereafter, a fine-tuning of %C, $A_0'$ and $A_1$ yields the final iteratively calculated values. Plotting $m_{\mathrm{inj-predicted}}$ versus $m_{\mathrm{inj-calculated}}$ yields one curve of all linear and cyclic injected mass values. The obtained slope and $r^2$ value of this curve should approach unity, indicating a good fit of the model. If not, other starting values should be tried. In Table 5 the result of this optimization procedure is given. As this $\chi^2$-optimization procedure works best with a large number of experiments, this procedure is probably less precise than the external universal calibration curve.

## 5. Conclusions

Under critical conditions the linear and cyclic structures of polyamide-6 were separated, identified and quantified. It was observed that an electrospray interface produced an unusable highly complex MS spectrum, due to multiply charged ions. Using MALDI-TOF-MS, the different series could be identified. Excellent separations of the linear and cyclic structures were obtained, although a slight mass

Table 3
Statistical data of the universal calibration curve with and without corrected areas

| | Universal calibration curve, without area correction | Universal calibration curve, with area correction |
|---|---|---|
| $\ln A_0'$ | 21.54 | 22.3 |
| $A_1$ | 1.17 | 1.19 |
| $R$ | 0.991 | 0.997 |

Table 4
Conversion of the areas of the linear and cyclic peaks with the standard deviation $\sigma$ to a corrected area with $\sigma = 1$. With these corrected areas and using the universal calibration curve the percentage of cyclic oligomers present in the polymer were calculated

| PA-6 | $m_{inj}$ (μg) | Area *L* (mV s) | Area *C* (mV s) | $\sigma$ (L) (s) | $\sigma$ (C) (s) | Corr. Area L | Corr. AreaC | *m* (L) calc. (μg) | *m* (C) calc. (μg) | % cyclic 100·m(C)/ {*m*(L)+*m*(C)} | % cyclic 100· *m*(C)/$m_{inj}$ | Recovery (%) |
|---|---|---|---|---|---|---|---|---|---|---|---|---|
| 16 | 19.1 | 4750 | 96 | 44 | 16 | 9950 | 165 | 17.9 | 0.58 | 3.13 | 3.01 | 96 |
| (a) | 59.0 | 19 000 | 345 | 49 | 13 | 41 000 | 575 | 58.3 | 1.64 | 2.74 | 2.79 | 102 |
| | 59.0 | 18 500 | 330 | 48 | 12 | 39 000 | 540 | 56.2 | 1.56 | 2.69 | 2.64 | 98 |
| | 125 | 47 000 | 865 | 51 | 13 | 100 000 | 1400 | 124 | 3.50 | 2.75 | 2.81 | 102 |
| | 226 | 100 000 | 1950 | 53 | 11 | 215 000 | 3150 | 236 | 6.83 | 2.81 | 3.02 | 108 |
| Mean | | | | | | | | | | 2.82 | 2.85 | 101 |
| 16 | 170 | 64 000 | 1400 | 51 | 14 | 136 862 | 2350 | 161 | 5.32 | 3.20 | 3.11 | 97 |
| (b) | 300 | 130 000 | 2950 | 53 | 13 | 282 914 | 4850 | 295 | 9.80 | 3.22 | 3.31 | 103 |
| | 470 | ≫ | 5450 | | 11 | | 8700 | | 16.0 | | 3.40 | |
| Mean | | | | | | | | | | 3.21 | 3.28 | 100 |
| 24 | 88 | 22 500 | 905 | 51 | 14 | 48 652 | 1500 | 67.6 | 3.71 | 5.20 | 4.20 | 81 |
| | 220 | 71 500 | 2550 | 49 | 14 | 152 329 | 4300 | 176 | 8.87 | 4.81 | 4.12 | 86 |
| | 530 | ≫ | 11 500 | | 13 | | 18 500 | | 30.3 | | 5.74 | |
| Mean | | | | | | | | | | 5.01 | 4.69 | 84 |
| 35 | 110 | 33 500 | 965 | 45 | 13 | 69 971 | 1597 | 91.6 | 3.87 | 4.05 | 3.55 | 87 |
| | 220 | 88 400 | 2350 | 44 | 13 | 185 167 | 3854 | 207 | 8.09 | 3.76 | 3.75 | 100 |
| Mean | | | | | | | | | | 4.27 | 4.00 | 94 |

dependence in the first (linear) peak was observed, indicating near-critical conditions.

With a direct spectrum of the polyamide, without preseparation of the linear and cyclic structures, doubts could arise about presence of the cyclics in the original sample, as they are generated in the mass spectrometer upon ionization. To the best of our knowledge, this is the first time that the cyclic

Table 5
Calculation of the percentage cyclic oligomers present in four different polyamides by using the iterative procedure

| Polyamide-6 | Initial values | | %C | Calculated $A_0'$ | Calculated $A_1$ | $\chi^2 \times 10^{10}$ | $r^2$ | Slope | %C |
|---|---|---|---|---|---|---|---|---|---|
| 16 (a) | | | | | | | | | |
| | $A_0'$ | $3.06\cdot10^{10}$ | 0 | $1.20\cdot10^{10}$ | 1.263 | 993 | 0.99 988 | 1.00 065 | 4.1 |
| | $A_{1\,average}$ | 1.227 | 5 | $1.21\cdot10^{10}$ | 1.263 | 993 | 0.99988 | 1.00061 | 4.1 |
| | | | 10 | $1.20\cdot10^{10}$ | 1.263 | 993 | 0.99988 | 1.00065 | 4.1 |
| 16 (b) | $A_0'$ | $2.45\cdot10^{10}$ | 0 | $1.17\cdot10^{7}$ | 0.703 | 370 655 | 0.95501 | 1.02791 | 0.1 |
| | $A_{1\,average}$ | 1.302 | 5 | $2.23\cdot10^{10}$ | 1.320 | 136 | 0.99999 | 1.00105 | 4.0 |
| | | | 10 | $1.22\cdot10^{16}$ | 2.389 | 86 892 | 0.97959 | 0.93599 | 7.5 |
| 24 | $A_0'$ | $1.00\cdot10^{10}$ | 0 | Error | Error | Error | Error | Error | Error |
| | $A_{1\,average}$ | 1.336 | 5 | $2.24\cdot10^{10}$ | 1.333 | 4801 | 0.99932 | 0.98918 | 6.9 |
| | | | 10 | $2.26\cdot10^{10}$ | 1.334 | 4801 | 0.99931 | 0.98899 | 6.9 |
| 35 | $A_0'$ | $5.24\cdot10^{10}$ | 0 | $5.28\cdot10^{10}$ | 1.398 | 253 | 0.99993 | 1.00383 | 5.3 |
| | $A_{1\,average}$ | 1.360 | 5 | $6.94\cdot10^{10}$ | 1.413 | 155 | 0.99999 | 1.00101 | 5.5 |
| | | | 10 | $7.05\cdot10^{10}$ | 1.414 | 155 | 0.99999 | 1.00090 | 5.5 |

pentacontamer (C50) is detected and identified.

It was shown that quantification of an ELSD chromatogram obtained at critical conditions is not straightforward and a peak width-area correction must be made to improve precision and accuracy. Furthermore, no molecular mass dependence was observed for the oligomers and polymers of the different series, although the provided calculation excludes the cyclic and linear monomer since their response deviated strongly from the higher oligomers. All polyamide samples analyzed contained a total of less than 7% cyclic oligomers.

## Acknowledgements

We gratefully acknowledge the management of DSM Research and DSM Division Fiber Intermediates for the permission to publish this work and the Institute for Mass Spectrometry of the University of Amsterdam (Professor Dr. N.M.M. Nibbering and R. Fokkens) for acquisition of the MALDI spectra

## References

[1] S.M. Aharoni, *n*-Nylons: Their Synthesis, Structure and Properties, Wiley, Chichester, 1997.
[2] S. Mori, Y. Nishimura, J. Liq. Chromatogr. 16 (1993) 3359.
[3] Z. Tuzar, P. Kratochvil, M. Bohdancky, Adv. Polym. Sci. 30 (1979) 118.
[4] G.v.d. Velden, J. Beulen, H. de Keijzer, Recl. Trav. Chim. Pays-Bas 110 (1991) 516.
[5] G.J. van Rooy, M.C. Duursma, C.G. de Koster, R.M. Heeren, J.J. Boon, P.J. Wijnand Schuyl, E.R.E.v.d. Hage, Anal. Chem. 70 (1998) 843.
[6] N. Nielen, Mass Spectrom. Rev. 18 (1999) 309.
[7] D. Muscat, H. Henderickx, G. Kwakkenbos, R. Van Benthem, C.G. de Koster, R. Fokkens, N.N.M. Nibbering, J. Am. Soc. Mass Spectrom. 11 (2000) 218.
[8] S.G. Entelis, V.V. Evreinov, A.V. Gorshkov, Adv. Polym. Sci. 76 (1986) 129.
[9] A.V. Gorshkov, H. Much, H. Becker, H. Pasch, V.V. Evreinov, S.G. Entelis, J. Chromatogr. A 523 (1990) 91.
[10] D. Berek, Macromol. Symp. 110 (1996) 33.
[11] V.V. Evreinov, A.V. Gorshkov, T.N. Prudskova, V.V. Gurýanova, A.V. Pavlov, A.Ya. Malkin, S.G. Entelis, Polym. Bull. 14 (1985) 131.
[12] B. Trathnigg, B. Maier, D. Thamer, J. Liq. Chromatogr. 17 (1994) 4285.
[13] V.V. Gurýanova, A.V. Pavlov, J. Chromatogr. 365 (1986) 197.
[14] A.V. Gorskov, V.V. Jevreinov, B. Lausecker, H. Pasch, H. Becker, G. Wagner, Acta Polym. 37 (1986) 740.
[15] H. Pasch, Macromol. Symp. 110 (1996) 107.
[16] H. Pasch, K. Rode, Polymer 39 (1998) 6377.
[17] D. Braun, E. Esser, H. Pasch, Int. J. Pol. Anal. Char. 4 (1998) 501.
[18] H.J.A. Philipsen, B. Klumperman, A.M. Herk, A.L. German, J. Chromatogr. A 727 (1996) 13.
[19] D. Berek, M. Janco, G.R. Meira, J. Polym. Sci. A: Polym. Chem. 36 (1998) 1363.
[20] G. Schultz, H. Much, R. Kruger, C. Wehrstedt, J. Liq. Chromatogr. 13 (1990) 1745.
[21] H. Pasch, B. Trathnigg, HPLC of Polymers, Springer, Berlin, 1999.
[22] H. Pasch, H. Kruger, H. Much, U. Just, Polymer 33 (1992) 3889.
[23] R. Kruger, H. Much, G. Schultz, Int. J. Polym. Anal. Character. 2 (1996) 221.
[24] R. Kruger, H. Much, G. Schultz, J. Liq. Chromatogr. 17 (1994) 3069.
[25] K.J. Wu, R.W. Odom, Anal. Chem. 70 (1998) 456A.
[26] R. Ghahary, M. Resch, H. Pasch, GIT Lab. J. 2 (1997) 96.
[27] R.M. Whittal, L.M. Russon, L. Li, J. Chromatogr. A 794 (1998) 367.
[28] M.W.F. Nielen, Anal. Chem. 70 (1998) 1563.
[29] H. Yun, S.V. Olesik, E.H. Marti, J. Microcol. Sep. 11 (1999) 53.
[30] Y. Mengerink, R. Peters, M. Kerkhoff, J. Hellenbrand, H. Omloo, J. Andrien, M. Vestjens, Sj. van der Wal, J. Chromatogr. A 878 (2000) 45.
[31] A.V. Gorshkov, S.S. Verenich, V.V. Evreinov, S.G. Entelis, Chromatographia 26 (1988) 338.
[32] A.V. Gorshkov, T. Overeem, V.V. Evreinov, H.A.A. van Aalten, Polym. Bull. 18 (1987) 513.
[33] L.R. Snyder, Chromatography, in: E. Heftmann (Ed.), 5th edition, Part A, Journal of Chromatography Library, Vol. 51A, Elsevier, Amsterdam, 1992.
[34] M. Abramowitz, I. Stegum, in: Handbook of Mathematical Functions, Dover, New York, 1970, p. 303.
[35] A. Stolyhwo, H. Colin, M. Martin, G. Guiochon, J. Chromatogr. 288 (1984) 253.
[36] M.L. Vestal, P. Juhasz, S.A. Martin, Rapid Commun. Mass Spectrom. 9 (1995) 1044.
[37] Y. Mengerink, R. Peters, M. Kerkhoff, J. Hellenbrand, H. Omloo, J. Andrien, M. Vestjens, Sj. van der Wal, H. Claessens, C.A. Cramers, in preparation.
[38] R. Puffr, V. Kubanek, in: Lactam-Based Polyamides, Vol. I: Polymerization, Structure and Properties, CRC Press, Boca Raton, FL, 1991.
[39] J.A. Loo, C.G. Edmonds, H.R. Udseth, R.D. Smith, Anal. Chem. 62 (1990) 693.
[40] R.D. Smith, J.A. Loo, R.R.O. Loo, M. Busman, H.R. Udseth, Mass Spectrom. Rev. 10 (1991) 359.
[41] R.D. Smith, J.A. Loo, C.G. Edmonds, C.J. Baringa Loo, H.R. Udseth, Anal. Chem. 62 (1990) 882.
[42] D.C. Schriemer, L. Liang, Anal. Chem. 68 (1996) 2721.

[43] Y. Mengerink, R. Peters, M. Kerkhoff, J. Hellenbrand, H. Omloo, J. Andrien, M. Vestjens, Sj. van der Wal, J. Chromatogr. A 876 (2000) 37.
[44] Y. Mengerink, S. van der Wal, H.A. Claessens, C.A. Cramers, J. Chromatogr. A 871 (2000) 259.
[45] C.G. de Koster, M.C. Duursma, G.J. van Rooij, R.M.A. Heeren, J.J. Boon, Rapid Commun. Mass Spectrom. 9 (1995) 957.
[46] G.J. van Rooij, M.C. Duursma, R.M.A. Heeren, J.J. Boon, C.G. de Koster, J. Am. Soc. Mass Spectrom. 7 (1996) 449.
[47] J.M. Charlesworth, Anal. Chem. 50 (1978) 1414.
[48] J.C. Miller, J.N. Miller, Statistics For Analytical Chemistry, Ellis Horwood, Prentice Hall, NY, 1993.